HHS Public Access

Author manuscript

IEEE Nanotechnol Mag. Author manuscript; available in PMC 2020 May 26.

Published in final edited form as:

IEEE Nanotechnol Mag. 2016 September ; 10(3): 12–20. doi:10.1109/MNANO.2016.2572243.

Nanocrystalline Diamond Electrodes:

Enabling electrochemical microsensing applications with high reliability and stability.

SHABNAM SIDDIQUI,
University of Arkansas, Fayetteville.

GAURAB DUTTA,
Bengal University of Technology, India.

CHAO TAN,
Donghua University, China

PRABHU UMASANKER ARUMUGAM
University of Arkansas, Fayetteville.

Abstract

THE DIAMOND (D) IS ONE OF the most precious materials in the world with unmatched physical and chemical properties, such as hardness, extreme chemical stability, high thermal conductivity, the highest acoustic velocity of any material, an extremely low friction coefficient when smooth, and nearly unmatched biocompatibility [1]. The carbon (C) atoms in Ds are tetrahedrally coordinated, i.e., each C atom is bonded to four others in the D lattice. This bonding is referred to as sp^3 bonding, and the strength and configuration of these bonds provide Ds with these unmatched fundamental properties and characteristics. Realizing these properties of the D in a C-based film that can easily be integrated into functional engineering systems and deployed in many applications has been a challenge for several decades. This is of primary concern in microelectronics, sensing, and hard-coating applications.

Graphical Abstract

In recent years, much progress has been realized in growing large-scale D films on a number of other important thin-film materials, such as silicon, silicon dioxide, and metals using well-established surface micropatterning techniques, which are also transforming D films into a very attractive engineering material for electrochemical (E) sensing. This article

shabnam@latech.edu.

focuses on the utilization of nanocrystalline D (NCD) films, their superlative properties, and the fabrication of E-sensing devices to harness these characteristics in application to biological and neurochemical sensing.

NCD

Over the past several decades, two-dimensional (2-D) films of synthetic Ds (Table 1) have been realized principally by employing chemical vapor deposition (CVD) methods. Ds grown on surfaces using CVD methods can be subdivided into two basic types: single crystal and polycrystal-line. The performance of single-crystal Ds, in many aspects, such as thermal conductivity, carrier mobility, and optical transparency, is superior to those of polycrystalline Ds (PCDs); however, the prohibitive cost and requirement for growth on D-only substrates seriously limits its application and commercialization. This article focuses on the use of PCD films grown using CVD methods because of its widespread use for E sensing.

In the 1990s, a new class of D material, NCD, emerged [2]–[6]. Its surface is composed of facets of the largest crystals that survived the nucleation process, which produces a surface roughness proportional to the film thickness. With its grain size, surface roughness, and thickness, all in the range of tens to hundreds of nanometers, the microfabrication and integration of these films into functional devices became a relatively straightforward task when compared to larger grained PCD or single-crystal Ds.

NCD has been reported to be composed of 99% sp^3-bonded C and therefore represents a phase-pure D film with essentially no graphitic (sp^2) C present. To be employed as an electrode material for sensing, the D is usually doped with nitrogen or boron (B) to enhance its electrical conductivity, leading to NCs that are n doped or p doped, respectively. The surfaces of these crystallites have significant pi-bonding and sp^2 hybridization, which is the principal reason that the film is not exactly 100% phase pure.

B-doped D (BDD) is broadly classified into three types based on its crystal-lite (grain) size: microcrystalline D (MCD), NCD, and ultra-NCD (UNCD) (Figure 1). MCD and NCD surfaces are generally rough with average R_a values of 500–1000-nm root mean square (rms) and ~5–100 nm, respectively, depending upon their thicknesses. Thicker films are substantially rougher.

Researchers at Argonne National Laboratory developed a near atomic-scale smooth UNCD film (R_a of ~5–8-nm rms) [7]. UNCD films have been proven to be very smooth, irrespective of thickness (i.e., they do not roughen as their thickness increases) [8], which should lead to less adsorption of nonspecific biomolecules in biological and neurochemical sensing and other biomedical applications. This additional advantage of UNCD can thus effectively remediate the surface fouling problems that plague other electrode materials for biosensing. Second, UNCD can be deposited over an extended temperature range (~350–800 °C) and thus can be more easily integrated with other thin-film processes [9]. Third, it can be deposited as a highly electrically insulating or a conducting (up to ~1,500 Ω^{-1} cm^{-1}) film by changing the gas mixture used [2]. Both NCD and UNCD electrodes are highly suitable

candidates for E biosensing and neurochemical sensing applications. Doped NCD films are an attractive electrode material to sense myriad of analytes.

NCD GROWTH

Hot filament CVD (HFCVD) and plasma-assisted CVD are two principal technologies available for manufacturing NCD films [10]. The NCD HFCVD process requires substrate surface temperatures of 400–950 °C to maintain high crystal quality for the deposited D films [11], [12]. Low-temperature and even room-temperature depositions have been reported [13], but films at these temperatures generally lack quality and exhibit poor deposition rates, film adhesion, and typically exhibit high film stresses. In HFCVD processes, a mixture of methane (CH_4) and hydrogen (H_2) is generally used with a CH_4/H_2 ratio of below 5%. Higher-purity NCD films (>99.9%) are achieved in a C-lean environment (<0.3%).

Besides the difference in gas chemistry, the growth mechanism for UNCD (typically used in our laboratory) is substantially distinct as compared to conventional NCD. UNCD has very frequent renucleation almost every 3–5 nm during film growth, which produces extremely low roughness, on the order of several nanometers [14]. In Raman spectra, a single 1,333-cm $^{-1}$ peak, representing a sp^3 D signature, dominates for single crystals and MCDs. As grain size decreases into the NCD range, the Raman spectra become more complicated [2]. NCD films are robustly grown on substrate materials that promote C formation, e.g., W, Ti, Si, SiC, Mo, and Nb [8], [15], [16]. These layers either assist the nucleation reaction with an incident D precursor species, such as methyl radicals, and/or enhance the bond between the substrate and/or reduce the thermal expansion differential between the D and its substrate.

Seeding is an essential pretreatment process for CVD D growth that provides reliable nucleation sites for film deposition. Major seeding methods include surface scratching, D-particle attachment, electrical biasing, and interlayer precoating. For the D-particle attachment methods, slurries of the D particles are sprayed or spin coated on a substrate, or the substrate is dipped into the slurries and/or treated with ultrasonic agitation. These methods are reliable and robust, and some of them can be used to coat the D on complex three-dimensional (3-D) substrates. Particularly with the introduction of ultradispersed D, the seed density on a substrate can be as high as 10^{11} cm^2.

A general understanding of CVD D-deposition mechanisms has been acquired over the years [17], [18]. Among the many types of reactions on the substrate surface, CH_x (x = 0–3) radicals react to form sp^2 and sp^3 bonds simultaneously, typically with the sp^2 bonds dominating. It is believed that high-temperature atomic H plays the key etch role to extract H from the CH bond on the surface to form H_2, which usually leaves behind a C-dangling bond so that a subsequent C atom from a radical precursor can react to continue the growth of the D-crystal lattice. At the same time, atomic H preferentially etches the sp and sp^2 sites, thus freeing up sites for sp^3 C reaction and growth, i.e., atomic H suppresses the growth of graphite and enhances the growth of the D. H-rich gas chemistry was quoted as a featured part of NCD synthesis (CH_4/H_2 < 5%), which differs from that of UNCD initialized with Ar-rich H_2 lean/free gas chemistry (CH_4/Ar = 1%). Another key point to note is that CH_4 is

not the only the C source that can be used, and there are actually several C-based organics, such as ethanol and methanol, that also can be used for D synthesis.

FABRICATION OF DOPED NCD MICROELECTRODES

For E-sensing applications, the ability to grow doped NCD films on various substrates and to subsequently pattern them into microelectrode (ME) and nanoscale electrode arrays is vital for achieving high spatiotemporal resolution, excellent sensitivity and selectivity, multiplexing capability, and low cost [19]–[21]. Such MEs are routinely fabricated by either using standard microfabrication techniques [19] (top–down approach) or employing nanomaterials [22] (bottom–up approach). For ultrasensitive sensor development, several groups, including ourselves, have used microlithographic techniques to fabricate well-defined reproducible ME geometries on BDD films [19], [23]. BDD coatings on microwires have been used for in vitro and in vivo neurochemical measurements [24], [25].

A typical fabrication process sequence for creating *p*-type BD NCD disk-shaped MEs is shown in Figure 2 (details are described in [19]). BD films are grown using gaseous trimethyl-B (TMB), diborane, or vaporized liquid trimethyl B [26]. High doping levels, i.e., $>10^{21}$ cm^3 or >3,000 ppm are used to provide adequate electrical conductivity (<0.1-Ω cm) for sensing applications. Generally, it was believed that dopant incorporation occurs in both grains and grain boundaries of conventional NCDs, whereas it mainly occurs in the grain boundaries of UNCDs [27]. Large-area NCD films can be patterned into microscale electrodes using standard semiconductor processing equipment.

NCD MEs have already demonstrated superior E stability, dimensional stability, low background currents, and a wide E potential window in aqueous media, which are all important for sensor technology development. UNCD ME arrays (MEAs) of varying sizes (250-to 10-μm in diameter) in a 3 × 3 MEA format [28] have been successfully employed by the current authors and others to detect a wide range of analytes including bacteria, neurochemicals, hormones, and heavy metals, among others (Figure 3) [19], [29]. Unlike other C electrodes that require elaborate time-consuming surface-cleaning steps, D electrodes require only a brief sonication in isopropanol prior to use. The aforementioned studies show minimal variation in current peak separation in cyclic voltammograms (Vs) from the nine MEs within the array and from array to array (<5%) demonstrating highly uniform reliable MEs with excellent E behavior.

ELECTRONIC PROPERTIES OF NCD

The E properties of the electrode controlling the transfer of charge between an electrode and an electrolyte are dependent on the electronic properties, such as the electrode’s resistivity, density of electronic states (DOS), conductivity, and background current/signal noise [30]. Electrode resistivity is the partially intrinsic property of the material as it depends upon its resistance and geometrical parameters, such as cross-sectional area and the length of the electrode, and therefore varies with different geometrical configurations of the electrode.

The DOS is more of an intrinsic property of the electrode and completely depends upon the material properties. Thus, it varies for different types of C materials. For example, the high

DOS for metals results from a large combination of atomic orbitals into the conduction and valence bands that overlap and cause electrons to move freely, leading to metallic conduction that follows Ohm's law. A higher DOS in an electrode increases the likelihood that an electron of the correct energy is available for electron transfer to the electrolyte so that the heterogeneous electron transfer rate is expected to be dependent on the DOS of the electrode material.

Crystalline D has a wide band gap of ~5.4 eV in a single crystal and is an effective insulator when undoped. NCD without the defects caused by doping has higher mobility than single-crystal Ds. Heavily BD NCD conducts electrons similar to metals due to its lack of a band gap. BD and sp^2-bonded C impurities are the two main factors that influence the conductivity of BDD films [31]. Higher BD leads to higher carrier concentration and increased conductivity. However, the lower DOS in doped D leads to lower conductivity than metals. The presence of sp^2-bonded C increases the V background current and decreases the working potential window. Additionally, the presence of this impurity affects the electron-transfer kinetics of redox systems differently.

For some redox systems, the presence of dopant impurities strongly accelerates the heterogeneous rate of electron transfer, whereas for others it has little effect on the kinetics. The background current of BDD films is considerably lower than conventional materials, thus resulting in high signal-to-noise ratios. This is highly advantageous for sensing, since low background noise would result in the detection of weak signals arising from a low concentration of analyte.

It is actually the background current that controls the limit of detection. The limit of detection is the minimum concentration of an analyte that is detectable, usually at a signal-to-noise ratio of three or greater. The low background current of D films arises from its lower capacitance and the absence of electroactive surface C–oxygen functional groups. Thus, by controlling the above-mentioned factors, it is possible to precisely fabricate MEs with the required surface conductivity, potential window, and background current required for sensing applications. Hence, BD NCD MEs have all the important E properties, such as low resistivity, high conductivity, right number of DOS, wide potential window, and low background current that are suitable for bio-and chemical sensing. NCDs possess excellent electronic properties that are reproducible and stable over the long term.

EIMPEDANCE SPECTROSCOPY-BASED NCD BIOSENSORS

Among the various classes of biosensors, molecular biosensors, such as E impedance spectroscopy (EIS) biosensors, have received widespread attention because of their potential for label-free detection [32]. Using this technique, a sensing biomolecule, such as an antibody or DNA, is immobilized on the conductive surface. The change in impedance due to the binding of a target, such as an antigen to a biomolecule, is rendered as a detection event. The sensitivity of detection depends upon the material properties of a target conductive surface, the immobilization process, and the interaction between the sensing biomolecule and the target.

There are two types of detection processes: *nonfaradaic* and *faradaic*. For a nonfaradaic process, the impedance change is mainly caused by a change in capacitance or the dielectric properties of the double layer, and no redox molecule is required. This approach is particularly useful when the conductivity of the functionalized surface is changed by the specific binding event and is more suitable for on-site diagnostics. For faradaic processes, the impedance change is caused by a change in resistance arising from the transfer of charge from a redox molecule [e.g., $Fe(CN)_6^{-3/-4}$] present in the solution. To attain high sensitivity, a DC potential is used that is usually equal to that of the open circuit potential applied to the electrode along with a small amplitude sinusoidal voltage. NCD electrodes offer a highly reproducible surface for reliable biosensing.

In a recent study, we used BD UNCD MEAs and EIS to demonstrate high selectivity with minimal nonspecific adsorption [19]. We presented an E pore circuit model to explain the EIS detection mechanism, along with a demonstration of improved signal reproducibility and increased sensitivity. By demonstrating improvements for the above-mentioned key issues, the use of UNCD for label-free EIS biosensing was realized. sp^3-bonded C atoms in UNCD and its intrinsically smooth surface (R_a < 10 nm) prevent bonding of interferents and thus minimize nonspecific adsorption. The differences in surface conductivity and bond structure of UNCD, i.e., less conductive homogenous grains and more conductive heterogeneous grain boundaries, ensure that the functionalization of such surfaces with TFAAD-dodecene monolayers and antibodies occur only with certain C bonds of Ds.

After functionalization, the electrode surface consists of two regions, one where the monolayers are formed with C atoms of the D and to which antibodies are attached, and the other area surrounding the antibodies that is covered with a casein blocker and acts as an insulator. Thus, a porelike structure is formed, and antibodies reside inside the pores. It is inside these regions where some part of the conductive electrode is exposed to the electrolyte and an exchange of electrons between the electrode and the electrolyte occurs. This exchange of electrons takes place only inside the pores because the remaining surface acts as an insulator. The addition of monolayers to the electrode surface reduces the E active surface, slows interfacial electron kinetics, and reduces the exchange current. The Nyquist plot of impedance spectra of such a modified surface was found to be a semicircle, which indicates a highly resistive interface. The high resistance is due to reductions in exchange current (I_0) and increases in charge-transfer resistance (R_{ct}). The relationship between I_0 and Rct for such a surface at nonequilibrium conditions is given by $R_{ct} = (1/\alpha f I_0) \log (I_0/I_0\text{eq})$, where F is the Faraday constant, α is the transfer coefficient, and I_0eq is the exchange current at equilibrium.

As evident from this equation, charge-transfer resistance is inversely proportional to the exchange current. Therefore, as the exchange current decreases, the impedance of the electrode surface is controlled by interfacial processes, and no diffusional characteristic is observed in impedance spectra. It was found that the impedance spectral data can be well simulated by a pore circuit model. The different elements of the circuit provide quantitative information on important parameters, such as the coverage and the density of the immobilized antibody, the uniformity of casein coverage, the electrolyte resistance inside and outside the pores, and the charge-transfer resistance.

The values of these parameters are then used to distinguish between a positive signal and a false positive signal. Currently, the research is geared toward collecting large data sets to optimize the parameters to obtain a highly reliable detection. It is notable that due to the unique properties of the UNCD interface, such as its chemical stability and ultrasmooth surface morphology, it facilitates the deposition of more uniform, dense, and conformal monolayers of casein. In addition, these UNCD surface characteristics produce a minimum of nonspecific binding, and a constant value of key sensor parameters, such as exchange current and charge-transfer resistance, can be repeatedly observed. Such excellent reproducibility and detection sensitivity are difficult or impossible to obtain with other types of electrode materials.

DIMENSIONALLY STABLE NCD MEs FOR NEUROCHEMICAL SENSING

An understanding of the human brain is probably the greatest intellectual challenge of the 21st century and beyond. Previous research in this highly topical field has demonstrated the importance of neurochemicals, such as dopamine (DA), glutamate, adenosine, and serotonin for neuronal communication in healthy and diseased states [33]. E techniques, such as fast-scan cyclic V (FSCV), offer a viable means of measuring neurochemicals rapidly with submillimeter and subsecond resolutions [34]. These methods routinely use the C fiber ME (CFM) (~5–10-μm diameter), which affords a spatial resolution in the micrometer domain [35] and, when combined with extended-scan FSCV, a detection limit of ~15 nM can be obtained in the brain.

Unfortunately, the increased sensitivity of extended-scan FSCV for CFM is at the expense of reduced response time due to rapid surface fouling. Nafion coatings and extended anodic waveforms [36] have been used to mitigate fouling and renew the surface, but they also decrease the electrode reactivity and degrade the CFM chemically. Also, it is not desirable to apply high anodic potentials (+1.4 V) in vivo as these can generate reactive oxygen species and cell death. This limits its use to acute measurements that measure neurochemicals in vivo for a few hours to a day. Thus, repeated FSCV measurements over months can be technically challenging.

On the contrary, NCD MEs with their superior dimensional stability could emerge as the next-generation electrode technology to detect chemicals “chronically” in the brain. Many studies have shown the many distinct advantages of NCD electrodes—i.e., extremely low background currents, excellent selectivity, biocompatibility, and superior dimensional stability for neurochemical detection [24], [25], [37], [38].

The ability to conformably coat NCD on microwires has encouraged researchers to consider NCD as an alternative to CFM. NCD microwire electrodes have been used successfully to detect neurochemicals in vivo using FSCV with sensitivities and response times comparable to CFM (Figure 4) [24]. It is important to note that ultrasmall electrodes, preferably in an array format, are sought for in vivo applications because of their requirement for high spatial–temporal resolution, minimal tissue damage/neuroinflammation, and multiplexing capabilities. Since sensitivity depends on surface area and surface chemistry, ultrasmall

electrodes exhibit reduced sensitivity because of less availability of adsorption sites and insufficient numbers of edge plane graphite sites.

One solution is to engineer novel 3-D ultrasmall electrodes that offer a high electrode and electroactive area. So, for the first time, we investigated the significance of UNCD electrode size on E properties [39]. Interestingly, as the UNCD ME size is reduced from 250 to 10 μm, impedance spectra change to two arcs, and each arc likely represents the impedance of grains and grain boundary phases, and only for ultra-MEs ($D \leq 25$-μm), microstructural and morphological defects, and surface oxygen groups are revealed in the spectra (Figure 5). This clearly demonstrates the effect of electrode size reduction on the E properties and, particularly, the critical role of grain boundary conductivity on the electrodes' E response.

Next, we improved the NCD kinetics and sensitivity toward DA by modifying the surface with 100–500-nm-thick C nanotube (CNT) layers. This new hybrid nanocomposite ME demonstrated a 127-fold increase in sensitivity (32 μAμM^{-1} cm^{-2}). In addition to an increase in sensitivity, the hybrid approach provides three other important benefits: First, CNTs can be selectively coated on MEs with a simple, scalable, and low-cost process, such as layer-by-layer assembly, CVD, and electrophoretic deposition. Second, the E properties can be precisely tuned by simply controlling the CNT film thickness. Third, remarkable improvements in DA sensitivity (>100-fold) and limits of detection (greater that tenfold) are demonstrated even when utilizing the same geometrical area for the NCD ME.

Finally, we also recently demon strated the superior dimensional stability of UNCD compared to a similar-sized CFM by directly measured comparative dimensional stability of these two materials. CFM was almost completely etched away after 40 h of E cycling (−0.4 to +1.4 V, 400 V/s, in a phosphate-buffered saline buffer), a cleaning procedure commonly used to renew a fouled CFM. In contrast, UNCD showed negligible etching under these conditions because of the greatly superior E stability of D surfaces.

In the future, a smaller ME (<10 μm), preferably a sp^3-sp^2 nanocomposite with a large electroactive area may be developed that will likely reduce neuroinflammation without comprising the detection sensitivity of the ME. The exceptional dimensional stability of NCD allows multiple cleanings of the fouled surface to realize chronic neurochemical monitoring.

SUMMARY AND OUTLOOK

NCDs could emerge as the next best electrode material for biological and neurochemical sensing because of the numerous advantages discussed in this article. Much progress is still required in the areas of integrating sensors into multifunctional multimodal systems and performing extensive field testing to validate the sensor stability and performance and its readiness to detect analytes in real-world environments.

Some of the key research directions that we believe are essential in realizing the full potential of the D biosensors are as follows:

1. the optimization of growth parameters for the deposition of D films at low temperatures to allow integration into established CMOS technologies and low-cost glass and polymer substrates
2. the development of protocols for reactivating biofouled NCD surface in situ in the brain for chronic neurochemical monitoring
3. the development of robust electrical circuit models that accurately detect analytes with fewer repeat experiments
4. finding the control parameters that one can use to tune the D grain and grain boundary phase properties specific to a given application.

How effectively knowledge is created in these new research directions will decide the timeline for the commercialization of a highly reliable and stable NCD microsensor for general use.

ACKNOWLEDGMENTS

We are grateful to Advanced Diamond Technologies, Inc. (Romeoville, Illinois) for their support over the years in developing UNCD films that were used for the sensing applications mentioned in this article. Prabhu Umasanker Arumugam acknowledges financial support from the Louisiana Board of Regents—RCS support fund (Contract. LEQSF(2014-17)-RD-A-07) and the assistance of Dr. J. Berg from the School of Design for the opening artwork.

Biography

Shabnam Siddiqui (shabnam@latech.edu) earned her B.S. and M.S. degrees in physics from the University of Delhi, India, and her Ph.D. degree in physics from the University of Arkansas, Fayetteville. She conducted her postdoctoral training at NASA Ames Research Center, California. She is currently a research assistant professor at the Institute for Micromanufacturing, Louisiana Tech University, Ruston. Her research interests are in understanding the electrochemical properties of nanomaterials and their application in sensing and energy storage.

Gaurab Dutta (gdu002@latech.edu) earned his B.Tech. degree in electrical engineering from West Bengal University of Technology, India. He is currently a Ph.D. student at the Advanced Materials Research Laboratory, Louisiana Tech. His current research focuses on developing a diamond electrochemical microsensor for chronic neurochemical monitoring.

Chao Tan (cta019@latech.edu) earned his B.S. degree in science and engineering of composite materials from Donghua University, China, and his M.S. degree in molecular science and nanotechnology from Louisiana Tech. He is currently a Ph.D. student at the Advanced Materials Research Laboratory, Louisiana Tech. His research interest is investigating carbon nanomaterials for electrochemical sensing.

Prabhu Umasanker Arumugam (parumug@latech.edu) earned his B.S. degree in mechanical engineering from PSG Tech, India; his M.S. degree in mechanical engineering; and his Ph.D. degree in microelectronics and photonics from the University of Arkansas, Fayetteville. He performed his postdoctoral training at NASA Ames Research Center, California. He is currently an assistant professor of mechanical engineering at the Institute

for Micromanufacturing and the director of the Advanced Materials Research Laboratory, Louisiana Tech University. His research focuses on carbon-nanomaterials-based electrochemical microtechnologies.

REFERENCES

[1]. Carlisle JA, "Diamond films: Precious biosensors," Nat. Mater, vol. 3, no. 10, pp. 668–669, 10 2004. [PubMed: 15467689]

[2]. Zeng H, Konicek AR, Moldovan N, Mangolini F, Jacobs T, Wylie I, Arumugam PU, Siddiqui S, Carpick RW, and Carlisle JA, "Boron-doped ultrananocrystalline diamond synthesized with an H-rich/Ar-lean gas system," Carbon, vol. 84, pp. 103–117, 4 2015.

[3]. Gruen DM, "Nanocrystalline diamond films," Annu. Rev. Mater. Sci, vol. 29, pp. 211–259, 8 1999.

[4]. Jiao S, Sumant A, Kirk MA, Gruen DM, Krauss AR, and Auciello O, "Microstructure of ultrananocrystalline diamond films grown by microwave Ar–CH_4 plasma chemical vapor deposition with or without added H_2," J. Appl. Phys, vol. 90, pp. 118–122, 2001.

[5]. Ashfold MNR, May PW, Rego CA, and Everitt NM, "Thin film diamond by chemical vapour deposition methods," Chem. Soc. Rev, vol. 23, pp. 21–30, 2 1994.

[6]. Gajewski W, Achatz P, Williams OA, Haenen K, Bustarret E, Stutzmann M, and Garrido JA, "Electronic and optical properties of boron-doped nanocrystalline diamond films," Phys. Rev. B, vol. 79, 045206, 1 2009.

[7]. Birrell J, Gerbi JE, Auciello O, Gibson JM, Johnson J, and Carlisle JA, "Interpretation of the Raman spectra of ultrananocrystalline diamond," Diam. Relat. Mater, vol. 14, no. 1, pp. 86–92, 1 2005.

[8]. Naguib NN, Elam JW, Birrell J, Wang J, Grierson DS, Kabius B, Hiller JM, Sumant AV, Carpick RW, Auciello O, and Carlisle JA, "Enhanced nucleation, smoothness and conformality of ultrananocrystalline diamond (UNCD) ultrathin films via tungsten interlayers," Chem. Phys. Lett, vol. 430, no. 4–6, pp. 345–350, 10 2006.

[9]. Xiao X, Birrell J, Gerbi JE, Auciello O, and Carlisle JA, "Low temperature growth of ultrananocrystalline diamond," J. Appl. Phys, vol. 96, no. 4, pp. 2232–2239, 8 2004.

[10]. Butler JE and Sumant AV, "The CVD of nanodiamond materials," Chem. Vap. Deposition, vol. 14, no. 7–8, pp. 145–160, July/Aug. 2008.

[11]. Potocky S, Kromka A, Potmesil J, Remes Z, Polackova Z, and Vanecek M, "Growth of nanocrystalline diamond films deposited by microwave plasma CVD system at low substrate temperatures," Phys. Status Solidi A, vol. 203, no. 12, pp. 3011–3015, 9 2006.

[12]. Wang T, Xin HW, Zhang ZM, Dai YB, and Shen HS, "The fabrication of nanocrystalline diamond films using hot filament CVD," Diamond Relat. Mater, vol. 13, no. 1, pp. 6–13, 1 2004.

[13]. Tsugawa K, Ishihara M, Kim J, Koga Y, and Hasegawa M, "Nanocrystalline diamond film growth on plastic substrates at temperatures below 100°C from low-temperature plasma," Phys. Rev. B, vol. 82, no. 12, pp. 125460, 9 2010.

[14]. Williams OA, Daenen M, D'Haen J, Haenen K, Maes J, Moshchalkov VV, Nesládek M, and Gruen DM, "Comparison of the growth and properties of ultrananocrystalline diamond and nanocrystalline diamond," Diamond Relat. Mater, vol. 15, no. 4–8, pp. 654–658, Apr.–Aug. 2006.

[15]. Michau D, Tanguy B, Demazeau G, Couzi M, and Cavagnat R, "Influence on diamond nucleation of the carbon concentration near the substrate surface," Diamond Relat. Mater, vol. 2, no. 1, pp. 19–23, 2 1993.

[16]. Haubner R, Lindlbauer A, and Lux B, "Diamond nucleation and growth on refractory metals using microwave plasma deposition," Int. J. Refract. Met. Hard Mater, vol. 14, no. 1–3, pp. 119–125, 2 1996.

[17]. Liu H and Dandy DS, "Studies on nucleation process in diamond CVD: an overview of recent developments," Diamond Relat. Mater, vol. 4, no. 10, pp. 1173–1188, 9 1995.

[18]. Chhowalla M, Ferrari AC, Robertson J, and Amaratunga GAJ, "Evolution of sp^2 bonding with deposition temperature in tetrahedral amorphous carbon studied by Raman spectroscopy," Appl. Phys. Lett, vol. 76, no. 11, pp. 1419–1421, 3 2000.

[19]. Siddiqui S, Dai Z, Stavis CJ, Zheng H, Moldovan N, Hamers RJ, Carlisle JA, and Arumugam PU, "A quantitative study of detection mechanism of a label-free impedance biosensor using ultrananocrystalline diamond microelectrode array," Biosens. Bioelectron, vol. 35, no. 1, pp. 284–290, 5 2012. [PubMed: 22456097]

[20]. Kiran R, Rousseau L, Lissorgues G, Scorsone E, Bongrain A, Yvert B, Picaud S, Mail-ley P, and Bergonzo P, "Multichannel boron doped nanocrystalline diamond ultramicroelectrode arrays: Design, fabrication and characterization," Sensors, vol. 12, no. 6, pp. 7669–7681, 6 2012. [PubMed: 22969367]

[21]. Hu J, Holt KB, and Foord JS, "Focused ion beam fabrication of boron-doped diamond ultra-microelectrodes," Anal. Chem, vol. 81, no. 14, pp. 5663–5670, 6 2009. [PubMed: 19545137]

[22]. Arumugam PU, Chen H, Siddiqui S, Weinrich JA, Jejelowo A, Li J, and Meyyappan M, "Wafer-scale fabrication of patterned carbon nanofiber nanoelectrode arrays: A route for development of multiplexed, ultrasensitive disposable biosensors," Biosens. Bioelectron, vol. 24, no. 9, pp. 2818–2824, 2 2009. [PubMed: 19303281]

[23]. Pagels M, Hall CE, Lawrence NS, Meredith A, Jones TG, Godfried HP, Pickles CS, Wilman J, Banks CE, Compton RG, and Jiang L, "All-diamond microelectrode array device," Anal. Chem, vol. 77, no. 11, pp. 3705–3708, 6 2005. [PubMed: 15924409]

[24]. Arumugam PU, Zeng H, Siddiqui S, Covey DP, Carlisle JA, and Garris P, "Characterization of ultrananocrystalline diamond microsensors for in vivo dopamine detection," Appl. Phys. Lett, vol. 102, no. 25, pp. 253107, 6 2013. [PubMed: 23918991]

[25]. Xie S, Shafer G, Wilson CG, and Martin HB, "In vitro adenosine detection with a diamond-based sensor," Diamond Relat. Mater, vol. 15, no. 2–3, pp. 225–228, Feb.–Mar. 2006.

[26]. Gajewski W, Achatz P, Williams OA, Haenen K, Bustarret E, Stutzmann M, and Garrido JA, "Electronic and optical properties of boron-doped nanocrystalline diamond films," Phys. Rev. B, vol. 79, no. 4, p. 045206, 1 2009.

[27]. Zapol P, Sternberg M, Curtiss LA, Frauenheim T, and Gruen DM, "Tight-binding molecular-dynamics simulation of impurities in ultrananocrystalline diamond grain boundaries," Phys. Rev. B, vol. 65, no. 4, p. 045403, 12 2001.

[28]. Arumugam PU, Siddiqui S, Zeng H, and Carlisle JA, "Nanocrystalline diamond biosensors," in Biosensors Based on Nanomaterials and Nanodevices, Li Jand Wu N, Eds. Boca Raton: CRC, Taylor & Francis Group, 2013, ch. 10, pp. 243,242–243,272.

[29]. Wakerley D, Güell AG, Hutton LA, Miller TS, Bard AJ, and Macpherson JV, "Boron doped diamond ultramicroelectrodes: A generic platform for sensing single nanoparticle electro-catalytic collisions," Chem. Commun, vol. 49, no. 50, pp. 5657–5659, 6 2013.

[30]. McCreery RL, "Advanced carbon electrode materials for molecular electrochemistry," Chem. Rev, vol. 108, no. 7, pp. 2646–2687, 6 2008. [PubMed: 18557655]

[31]. Szunerits S, Nebel CE, and Hamers RJ, "Surface functionalization and biological applications of CVD diamond," MRS Bull, vol. 39, no. 6, pp. 517–524, 6 2014.

[32]. Daniels JS and Pourmand N, "Label-free impedance biosensors: Opportunities and challenges" Electroanalysis, vol. 19, no. 19, pp. 1239–1257, 5 2007. [PubMed: 18176631]

[33]. Swanson CJ, Bures M, Johnson MP, Linden A-M, Monn JA, and Schoepp DD, "Metabo-tropic glutamate receptors as novel targets for anxiety and stress disorders," Nat. Rev. Drug Discov, vol. 4, no. 2, pp. 131–144, 2 2005. [PubMed: 15665858]

[34]. Clark JJ, Sandberg SG, Wanat MJ, Gan JO, Horne EA, Hart AS, Akers CA, Parker JG, Willuhn I, Martinez V, Evans SB, Stella N, and Phillips PEM, "Chronic microsensors for longitudinal, subsecond dopamine detection in behaving animals," Nat. Methods, vol. 7, no. 2, pp. 126–129, 2 2010. [PubMed: 20037591]

[35]. Robinson DL, Hermans A, Seipel AT, and Wightman RM, "Monitoring rapid chemical communication in the brain," Chem. Rev, vol. 108, no. 7, pp. 2554–2584, 6 2008. [PubMed: 18576692]

[36]. Takmakov P, Zachek MK, Keithley RB, Walsh PL, Donley C, McCarty GS, and Wightman RM, "Carbon microelectrodes with a renewable surface," Anal. Chem, vol. 82, no. 5, pp. 2020–2028, 2 2010. [PubMed: 20146453]

[37]. Sarada BV, Rao TN, and Tryk DA, and Fujishima A, "Electrochemical oxidation of histamine and serotonin at highly boron-doped diamond electrodes," Anal. Chem, vol. 72, no. 7, pp. 1632–1638, 3 2002.

[38]. Park J, Quaiserová-Mocko V, Pecková K, Galligan JJ, Fink GD, and Swain GM, "Fabrication, characterization, and application of a diamond microelectrode for electrochemical measurement of norepinephrine release from the sympathetic nervous system," Diamond Relat. Mater, vol. 15, no. 4–8, pp. 761–772, Apr.–Aug.2006.

[39]. Dutta G, Siddiqui S, Zeng H, Carlisle JA, and Arumugam PU, "The effect of electrode size and surface heterogeneity on electrochemical properties of ultrananocrystalline diamond microelectrode," J. Electroanal. Chem, vol. 756, pp. 61–68, 11 2015.

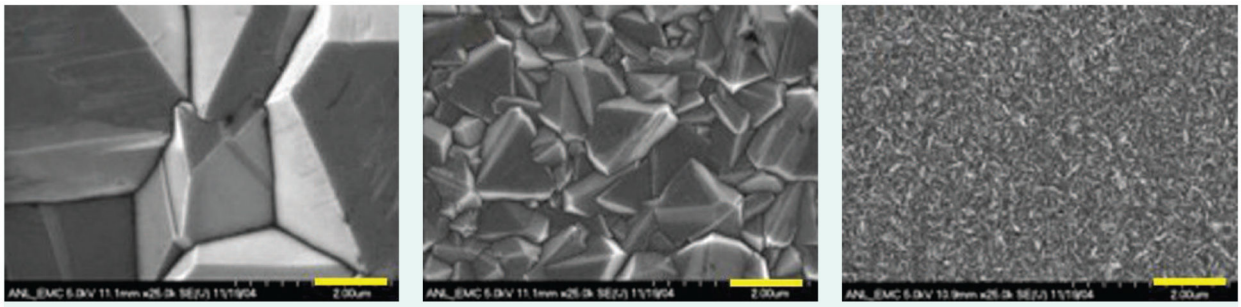

FIGURE 1.

The classification of BD D films: scanning electron microscopy (SEM) images of (a) MCD, (b) NCD, and (c) UNCD. The scale bar is 1 μm.

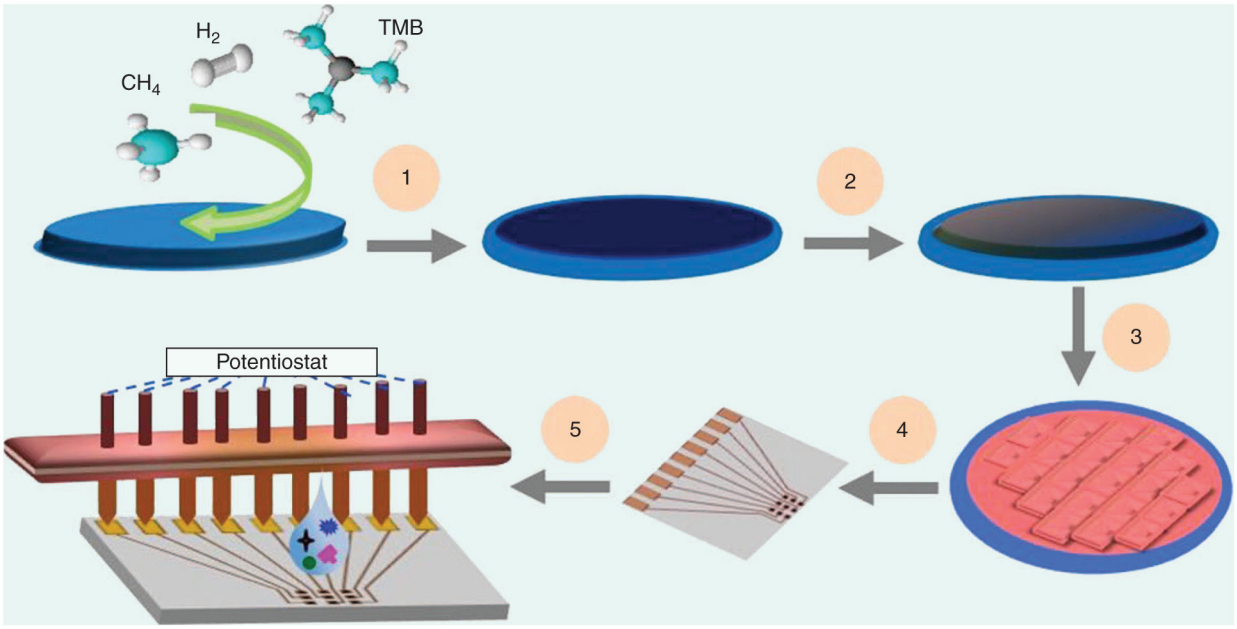

FIGURE 2.

A schematic of the wafer-scale microfabrication of NCD ME arrays. (1) Hot filament CVD deposition of a BD NCD film on an Si/SiO_2 wafer. (2) Plasma-enhanced CVD deposition of SiO_2. (3) Photolithography micropatterning of oxide, dry etching micropatterning of NCD, and wet etching of SiO_2 to expose NCD MEs and electrical contact pads. (4) Dicing into individual chips with nine MEs patterned into 3 × 3 arrays. (5) An E sensor test bed. The details have been reported elsewhere [19].

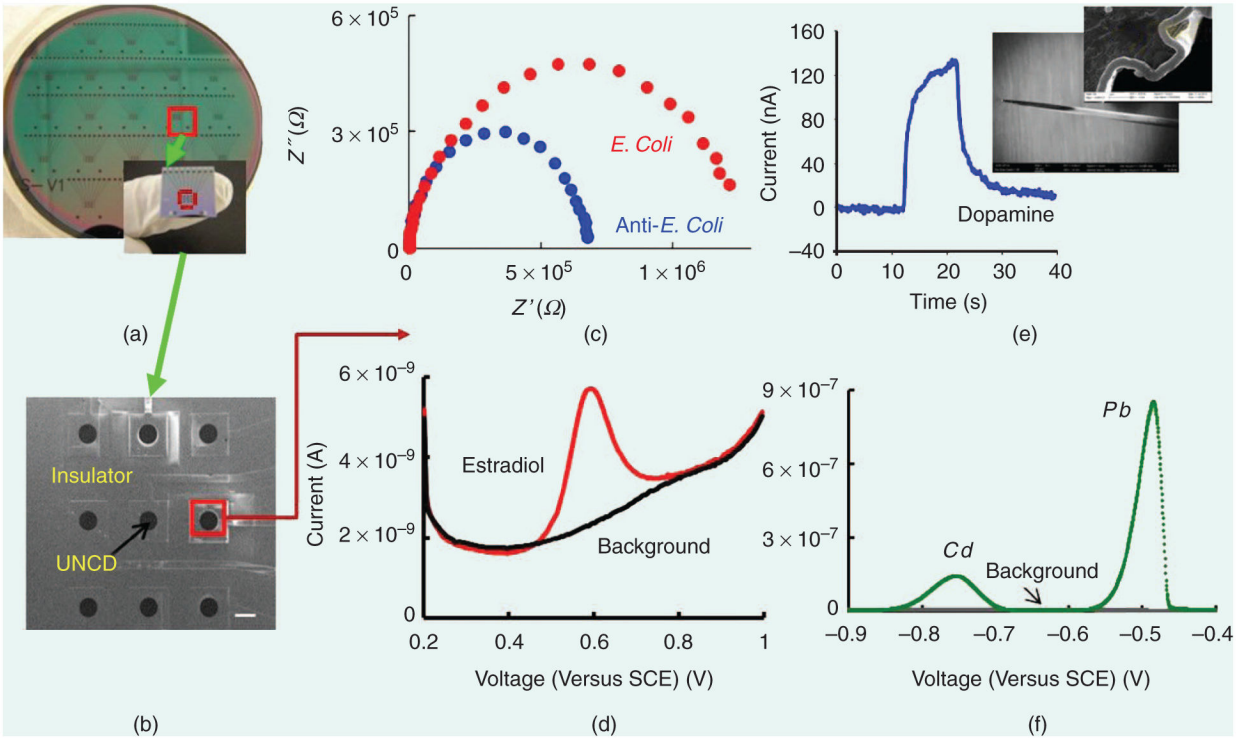

FIGURE 3.

The biological and chemical sensing applications of UNCD MEs: (a) An optical image of a UNCD planar 3 × 3 MEA fabricated in a 4-in silicon wafer. (b) An SEM image of one of the chips showing the nine individually addressable MEs (scale bar: 200 μm). (c) E detection of *E. coli* K12 bacteria. A Nyquist plot obtained after antibodies and after bacteria capture. (d) Differential pulse V (DPV) detection of 17-estardiaol (3 ppm), a hormone in a pharmaceutical wastewater stream.(e) Flow injection analysis of DA (10 μM) on an UNCD-coated tantalum microwire (inset, SEM image). (f) DPV detection of heavy metals (Cd,Pb) 5-ppm each.

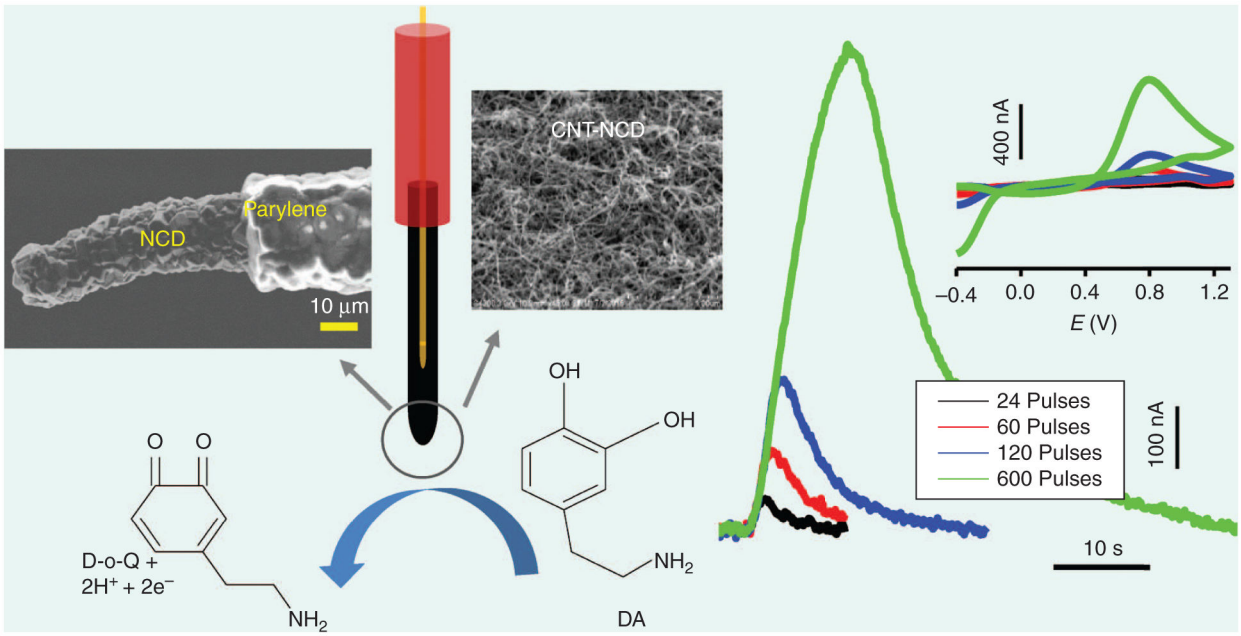

FIGURE 4.

The concept and use of unmodified and CNT-modified D MEs for in vivo and in vitro DA measurements have been reported elsewhere [24].

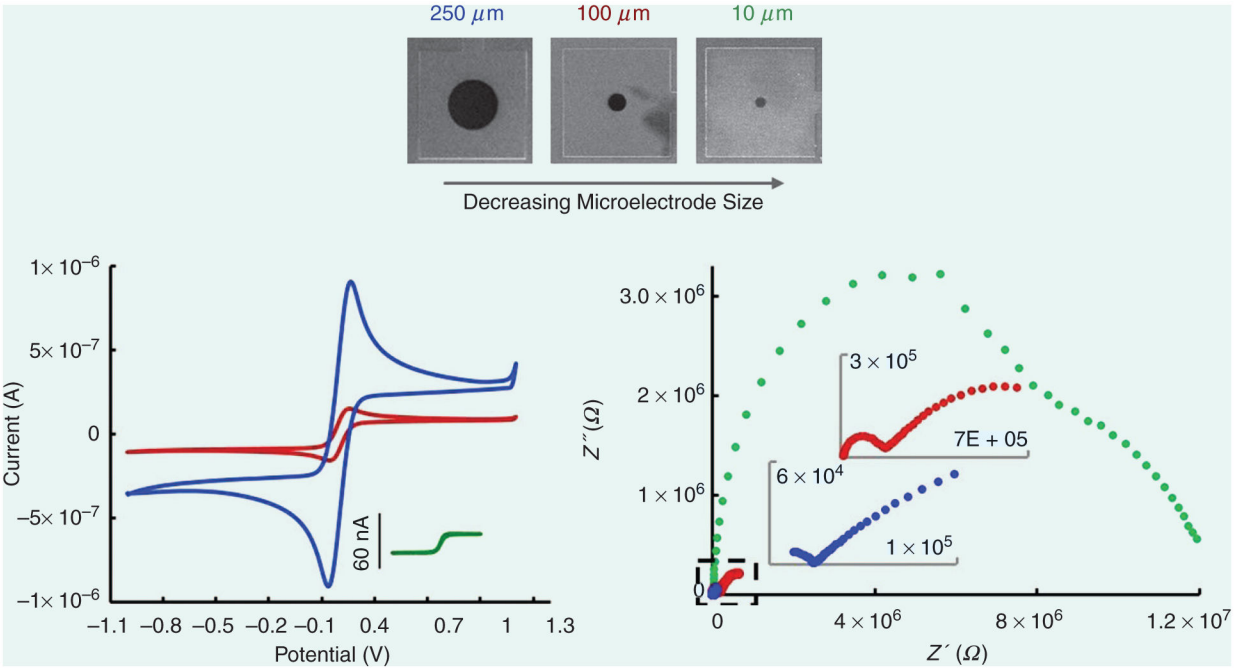

FIGURE 5.

The cyclic Vs (CVs) and Nyquist plots of 10-μm, (green), 100-μm (brown), and 250-μm UNCD (blue) MEs. The electrolyte is 5-mM Fe(CN)63−/4− in 1-M KCl. The scan rate for the CV is 100 mV/s. EIS spectra taken at 0-mV amplitude, 0.1 Hz–100 KHz. Details reported elsewhere [39].

TABLE 1

The properties of the D [1].

PROPERTIES	CVD D
Hardness	10,000 kg mm^{-2}
Thermal conductivity	20 Wm^{-1} K^{-1} (at 300 K)
Electron mobility	4,500 cm^2 V^{-1} s^{-1}
Hole mobility	3,800 cm^2 V^{-1} s^{-1}
Band gap	5.47 eV
Density	3.52 g cm^{-3}
Melting point	4,027 °C
Resistivity	10^{20} W cm
Bond length	1.54 A°
Bond angle	109.47°
Bonding	sp^3
Dielectric constant	5.7
Refractive index	2.41 (at 591 nm)